ELSEVIER

Heat transfer from an obliquely impinging circular air jet to a flat plate

Xiaojun Yan and Nader Saniei
Department of Mechanical and Industrial Engineering, Southern Illinois University at Edwardsville, Edwardsville, IL, USA

A series of experiments was conducted for the measurement of local convective heat transfer coefficients for an obliquely impinging circular air jet to a flat plate. In the experiments, the oblique angles selected were 90°, 75°, 60° and 45°, with 90° being a vertical jet. Two different Reynolds numbers of 10,000 and 23,000 were considered for the purpose of comparison with previous data available in the literature. Another parameter varied in the measurements was the dimensionless jet-to-plate distance, L/D. Four values of L/D(2, 4, 7, and 10) were considered in the experiments. The experiments were conducted using the preheated wall transient liquid-crystal technique. Liquid-crystal color changes were recorded with a video system. Local convective heat transfer coefficients were obtained through the surface transient temperatures that were related to the recorded color information. Detailed local heat transfer coefficients were presented and discussed in relation to the asymmetric wall jet upon impingement of the jet flow. Results of experiments show that, for a given flow situation, the point of maximum heat transfer shifts away from the geometrical impingement point toward the compression side of the wall jet on the axis of symmetry. The shift is more pronounced with a smaller oblique angle (larger jet inclination) and a smaller jet-to-plate distance. Comparisons of experimental results with existing heat transfer data for both obliquely impinging jets and vertical impinging jets are made. The effect of oblique angles on heat transfer was assessed.

Keywords: heat transfer; obliquely impinging jet; liquid-crystal technique

Introduction

Impinging fluid jets have been widely used in many industrial processes, such as paper drying, glass tempering, gas turbine blade cooling, and electronic cooling. The complex nature of a turbulent impinging jet flow, a jet issuing out of a pipe or nozzle and then impinging on a target surface with change of flow direction upon impingement, makes it difficult to rely on analytical solutions to predict the heat transfer process between the jet and the target plate. Experimental work has been necessary in this area to evaluate and predict the characteristics of heat transfer.

Collections of literature on impinging jet heat transfer are available and reviewed by Downs and James (1987), Jambunathan et al. (1992), and Viskanta (1993). The majority of studies have focused on jet impingement on flat surfaces with a single or multiple vertical impinging jets. Fluid flow and heat transfer characteristics from a single vertical impinging jet to a flat surface have been well established for different jet nozzle shapes. The flow field is normally considered to have three regions: the free jet region; the stagnation region; and the wall jet region. The common features are the very localized enhancement of heat transfer in the stagnation region and a radial heat transfer distribution in the wall jet region according to the type of boundary-layer buildup on the surface.

For a vertical circular jet impinging on a flat plate, it was concluded from early experimental results (Gardon and Akfirat 1965) that, for the stagnation region, the maximum heat transfer happens at a jet-to-plate distance of about six times the jet diameter. The radial heat transfer distributions show either a monotonic decrease or, with a secondary maximum at a radial distance from the stagnation point of R/D about two for particular Reynolds numbers and small jet-to-plate distance ($L/D < 6$). These are further confirmed by many other researchers as reviewed also by Martin (1977) and Hrycak (1983).

Impinging jets with an oblique angle (non-vertical jets) happen in many applications. The imposed complexity attributable to the oblique angles in the fluid flow and heat transfer could add to the problem of nonuniform heating or cooling of impinging jets in industrial processes. It is, therefore, important to understand the effect of obliqueness of an impinging jet to the heat transfer process.

Many studies have investigated the effect of jet oblique angles on the flow field. Beltaos (1976) investigated the wall pressure and shear stress in the impingement region of an oblique circular turbulent jet. His nozzle Reynolds number ranged from 35,000 to

Address reprint requests to Professor Xiaojun Yan, Department of Mechanical and Industrial Engineering, Southern Illinois University at Edwardsville, Edwardsville, IL 62026-1805, USA.

Received 4 February 1997; accepted 28 May 1997

Int. J. Heat and Fluid Flow 18: 591–599, 1997

655 Avenue of the Americas, New York, NY 10010

0142-727X/97/$17.00
PII S0142-727X(97)00051-9

100,000, and jet-to-plate distance (L/D) was in the range of 15–47. The experimental results showed a "quasi-axisymmetric" feature of the flow field; i.e., the shear stress components normal to the radial plane (θ direction) was small. The location of stagnation pressure was shifted away from the geometrical impingement point. The amount of a shift was well correlated to semi-empirical pressure length scales based on surface static pressure distributions. Only few studies have been done on the heat transfer of obliquely impinging jet. Sparrow and Lovell (1980) used the naphthalene mass-transfer technique studied the heat transfer characteristics of an obliquely impinging circular air jet on a flat surface. Their Reynolds number based on the jet orifice varied from 2500 to 10,000 and jet-to-plate distance was in the range of 7–15. Their results showed that the maximum point of heat transfer was shifted from the geometrical impingement point along the axis of symmetry. They concluded that the maximum heat transfer and average heat transfer were not highly sensitive to the oblique angle of the jet. However, the distributions of local heat transfer coefficients in radial directions were rather nonuniform, with the compression slide ("uphill" side) decreasing more rapidly than that on the "downhill" side along a radial direction. Goldstein and Franchett (1988) used metallic foil heaters with liquid crystals to measure the local heat transfer from an oblique jet to a flat plate. The impinging jet was issued from a square-edge orifice with three Reynolds numbers (10,000, 20,000, and 30,000). Their jet-to-plate distance varied from 4 to 10. A heat transfer correlation was developed for the Nusselt number as a function of the jet oblique angle and jet-to-plate distance. Ichimiya and Nasu (1993) measured the local heat transfer distribution of an oblique jet impinging on a surface. Their experiment was conducted only for one small jet-to-plate distance ($L/D = 1$), and there was no wall jet region after impingement because of a confinement surface parallel to the test plate.

There is also interest in the application of fan-powered vertical take-off and landing (VTOL) vehicles where the flow field can be simulated by an obliquely impinging circular air jet flow. Some typical numerical simulations of flow field and heat transfer using k–ε turbulence model included Hwang et al. (1982), Hwang and Tsou (1983), and Chuang and Wei (1991). In these cases, very large jet-to-plate distance and high Reynolds numbers were used.

The objective of this study is to investigate the effect of oblique angle on the local convective heat transfer distribution on a flat plate for an obliquely impinging circular air jet. The experimental parameters are the Reynolds number (10,000 and 23,000) based on the jet exiting condition, jet-to-plate distance ($L/D = 2$, 4, 7, and 10), and the oblique angle (90°, 75°, 60°, and 45°), with 90° being the conventional vertical jet where existing data can be used for comparisons. The Reynolds number is chosen so that the temperature of the jet is the same as the ambient temperature. The experimental method used in this study is the preheated wall transient technique with the use of liquid crystals, which was previously developed for the accurate measurement of local heat transfer coefficients.

Experimental technique and facilities

Preheated wall transient liquid-crystal technique

The preheated wall transient liquid-crystal technique has proved to be an accurate method for detailed local convective heat transfer coefficient measurement (see Baughn et al. 1989, 1994). The technique provides local heat transfer information as well as flow field information through the color change of thermochromic liquid crystals coated on the surface under study.

The basic principle of the transient liquid-crystal technique is to evaluate the local heat transfer coefficient from two measurements: (1) a measured temperature difference (surface to fluid); and (2) the transient time period for this difference to occur. Descriptions of the transient technique can be found in Ireland and Jones (1986), Metzger and Larson (1986), O'Brien et al. (1986), Jones and Hippensteele (1987), Saabas et al. (1987), and Metzger et al. (1991). Based on similar measuring methodology, Baughn and Yan (1991) developed the preheated wall liquid-crystal technique. It has been applied to external as well as internal heat transfer situations.

By choosing a test surface with low thermal diffusivity, the surface heat conduction in the transient process is normally assumed to be limited to a very thin layer near the surface and a simple one-dimensional (1-D) analytical solution for transient heat conduction can be used. The 1-D, transient surface heat conduction problem with a time invariant total local heat transfer coefficient h_t (boundary condition of third kind) has the solution (see Carslaw and Jaeger 1959)

$$\frac{T_w - T_\infty}{T_{w,i} - T_\infty} = e^{\gamma^2}\mathrm{erfc}(\gamma) \tag{1}$$

$$\gamma = \frac{h_t\sqrt{t}}{\sqrt{(\rho C_p k)_w}} \tag{2}$$

Notation

C_p	specific heat, kJ/kg-K
D	diameter of the impinging jet, m
erfc	complementary error function
h	heat transfer coefficient, W/m^2-K
k	thermal conductivity, W/m-K
L	jet-to-plate distance, m
O	geometrical impingement point (in Figure 2)
r	radial coordinate of jet at issuing plane, m
R	radial coordinate of the surface, m
Re	Reynolds number based on jet exit velocity and the jet diameter D
S	shift of point of maximum heat transfer from the geometrical impingement point, m
t	time, s
T	temperature, K
TI	turbulent intensity, %
V	velocity, m/s
Z	coordinate along jet issuing direction, m

Greek

γ	nondimensional parameter, defined by Equation 2
θ	surface directional angle, °
ρ	density of the surface, kg/m^3
Φ	oblique angle of the jet, °

Subscripts

i	initial
lc	liquid crystal
o	jet exit
t	total
w	wall
∞	ambient

In the above equation, T_∞ is the temperature of the ambient fluid. The wall temperature changes from its initial value $T_{w,i}$ to a temperature $T_w(t)$ at a particular time t during the transient process.

In the preheated wall transient technique, the total local heat transfer coefficients h_t and the wall temperature $T_w(t)$ in Equation 1 is determined based on the liquid-crystal color change. The time t to reach this temperature for the surface is measured using a video system. Equation 2 is used to determine the total local heat transfer coefficient at a particular location. The convective heat transfer coefficient is deduced from the total heat transfer coefficient by using a radiation heat transfer coefficient. The radiation correction was made by assuming that the test plate was viewing a large hemispheric space at room temperature. A mean surface temperature of $0.5(T_{w,i} + T_{lc})$ and a surface emissivity of 0.7 was used for the calculation.

Digital color image acquisition and processing

The image acquisition system consists of a video camera, NTSC time code generator, S-VHS tape recorder, and a monitor. The liquid-crystal color change (as an indicator of surface temperature) is recorded and played back. A particular color change is calibrated as the temperature to be measured. For a given time, a series of color patterns (e.g., elliptical rings in the case of oblique circular jet) indicates a series of isotherms and thus iso-h (heat transfer coefficients) lines.

During a test run, the color change of the liquid crystals on the surface of the test section is recorded by the video camera system. The video system consists of a CCD camcorder (Zenith, VM7170, NTSC), a fiber optical Halogen illuminator (Techni-Quip, T-Q/FOI-1), a TV monitor, and an S-VHS recorder (JVC, BR-S378U). The camera is situated at a 45° angle with the horizontal plane of a vertical jet. The viewing direction is normal (on $\theta = 90°$ line) to the plane of symmetry ($\theta = 0°-180°$). Video frames of a dummy test plate with a marked polar coordinate system was produced immediately before a test run. With all the conditions held the same (camera angle, light angle, etc.), the test run is then performed. In this way, the effect of geometric distortion on the video is eliminated.

The recorded video image of liquid-crystal color for a given time is then captured by a true-color image processing unit (PC-Pentium with a Coreco 24-bit true-color card). The composite image is analyzed in red, green, and blue (RGB) and hue, saturation, and intensity (HSI) color spaces. The color information, thus, translates into local temperature information for the given time. The local temperature and time data are used to determine the local heat transfer coefficients. The calibration procedure of color *versus* temperature was similar to that of Camci et al. (1993) and was described in detail in Yan et al. (1995) and Yan and Saniei (1996).

Facilities

The experimental setup is shown in Figure 1. The major components of the experimental facilities are a blower, one long pipe, and a test plate coated with liquid crystals (BM/R35C1W/C17-10, Hallcrest, Inc.). The pipe is made of PVC with an inside diameter of 2.05 cm and a total length of 60 pipe diameters. It is desirable to have velocity distributions of fully developed pipe flows and the temperature uniform across the pipe at the jet exit. The test plate is made of Plexiglas with a thickness of 6.35 mm and the heat transfer active area (liquid-crystal coating) is 15×23 cm^2.

The test plate was placed in a specially designed constant temperature heating box controlled by a PC-based data acquisition system (Strawberry Tree, Mini-16). The test plate was placed in the box for a long period of time before the temperature of the test plate is uniform. The test plate was then quickly removed from the oven and placed in position under the jet, with an insulation plate covering it. The fast removal of the insulation plate initiated the transient process. The color change at a given location occurred at a given time. As the test plate was cooled down by the jet flow, a color band swept through the surface and the whole process was recorded on video tapes.

A Pitot tube and a hot-film sensor (TSI, T1210) with an anemometer system (TSI, FlowPoint) were used for velocity and turbulent intensity measurements.

A standard uncertainty analysis as described by Kline and McClintock (1953) was performed for the experimental results. The uncertainty in the local heat transfer coefficients ranges from 3.5% to 8.0%. The largest contribution to the uncertainty is from the measurement of the time for the color change to occur.

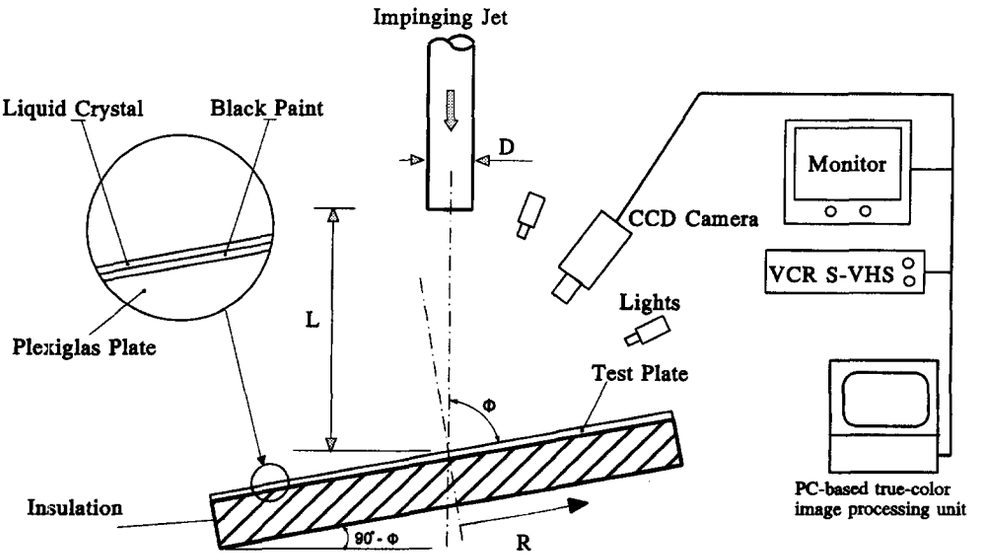

Figure 1 Experimental apparatus

Results and discussion

Detailed local heat transfer coefficients are obtained to evaluate the effect of oblique angle on the local heat transfer in both stagnation and wall jet regions. The experiments are performed for Reynolds number of 10,000 and 23,000 and jet-to-plate distance (L/D) of 2, 4, 7, and 10. To facilitate the understanding of the results in following discussions, a brief description of the coordinate system is appropriate.

Figure 2 shows the coordinates used in this study. The whole heat transfer surface can be divided into two symmetric regions. The plane of symmetry is the plane intersecting $\theta = 0°$ and $\theta = 180°$, the principal axes. Point O is the geometrical impingement point and point S is the point of maximum heat transfer. The distributions of local heat transfer results are presented along seven radial directions, $\theta = 0°$, 30°, 60°, 90°, 120°, 150°, and 180°. For jet characteristics, a Z coordinate is used that starts from the edge of the jet issuing plane, pointing toward the surface.

Jet flow characteristics

Centerline velocities and turbulent intensity of the jet are shown in Figure 3 for the range of z/D up to 10. The measurement was performed for a free jet. It shows that the centerline momentum of the jet decays by ~ 10% from that at the exit by a distance of six diameters away from the exit, which is normally considered the potential core of a jet. The turbulent intensity in the centerline picks up rapidly beyond a distance of four diameters. The traverse profiles of velocity and turbulent intensity of the jet were found to be typical of those for a turbulent pipe flow (Figure 4).

Point of maximum heat transfer

In transient measurement, the point of maximum heat transfer on the surface was readily measured by the fact that the highest heat transfer corresponds to the shortest time for the color change to happen. The shift of maximum heat transfer from the geometrical impingement point was found toward the compression side on the principal axes. The results are shown in Figure 5 for Reynolds number of 23,000. Notice the scale change for the lower portion in the figure.

Figure 5 is the plot of the shift of maximum heat transfer scaled by the jet-to-plate distance. The effect of oblique angles on the shift of maximum heat transfer is found to be sensitive to the jet-to-plate distance for the jet-to-plate distance range measured. As the jet moves away from the plate ($L/D > 6$), the well-mixed free jet flow has a more uniform momentum before impinging on the surface. The effect of oblique angles becomes minimum with large L/D. This is consistent with the surface stagnation pressure measurements of Beltaos (1976), where very large jet-to-plate distance ($L/D = 15$–47) was used. Sparrow and Lovell's (1980) mass/heat transfer result is also shown in Figure 5. Their heat transfer results show the insensitivity of L/D to the shift of point of maximum heat transfer for the range of $7 \leq L/D \leq 15$. The deviation in the comparison of present data to Sparrow and Lovell can be explained by differences in the jet-to-plate distance. Based on observations of others, Sparrow and Lovell argued that for a complex turbulent flow, such as the impinging jet flow, the asymmetric momentum transport process associated with a skewed velocity field is responsible for the "displacement of maxima or minima of related quantities." They speculated that the position of maximum pressure (Beltaos' definition of stagnation point) might not be the same point as the stagnation point (zero velocity), and neither might they coincide with the point of maximum mass/heat transfer point. It can be stated that the correlations between the positions of local maximum of pressure, local maximum of heat transfer and the stagnation point is unclear. Only through coordinated experimental work of measuring surface pressure, velocity field and heat transfer for the same jet configuration could it be resolved.

As a result of this study, however, for applications of obliquely impinging jet heat transfer with a small jet-to-plate distance, the shift of point of maximum heat transfer is sensitive to the jet-to-plate distance, and the assessment of nonuniform heating or cooling becomes more important. Figure 6 shows the shift of point of maximum heat transfer for a fixed jet-to-plate distance $L/D = 7$ for two Reynolds numbers 10,000 and 23,000. For the lower-Reynolds number of 10,000, the shift of maximum heat transfer is observed consistently less than that of the higher-Reynolds number. This is opposite to the trend in Figure 5 when comparing with results of Sparrow and Lovell (1980) where their Reynolds number was in the range of 2500 to 10,000. They found that the shift of maximum mass/heat transfer is insensitive to Reynolds number for the range used. The difference could be explained by the types of jet and flow patterns used. The current experiment uses a blowing type jet issuing out of a fully developed pipe flow. The mixing of free jet with the ambient is more pronounced in higher-Reynolds numbers as compared to Spar-

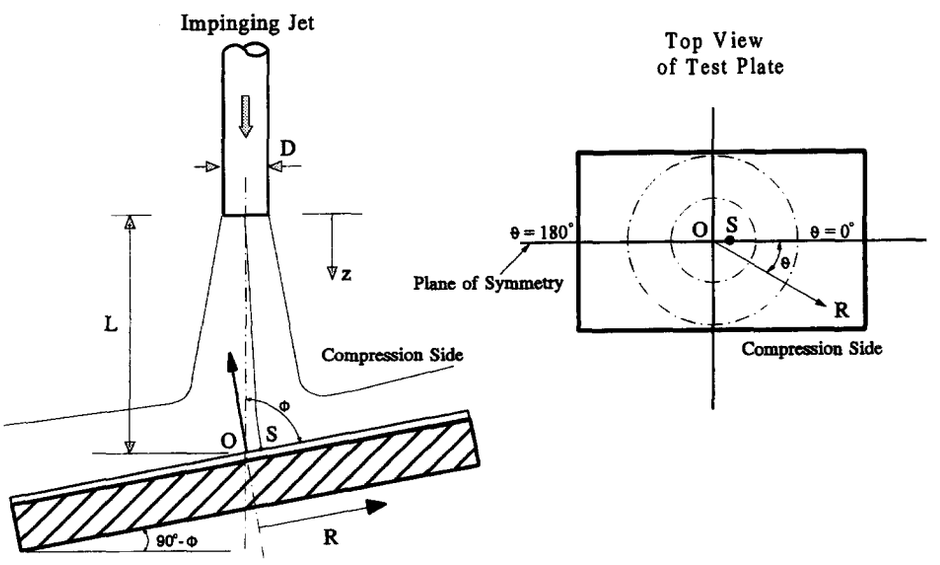

Figure 2 Coordinate system of the surface

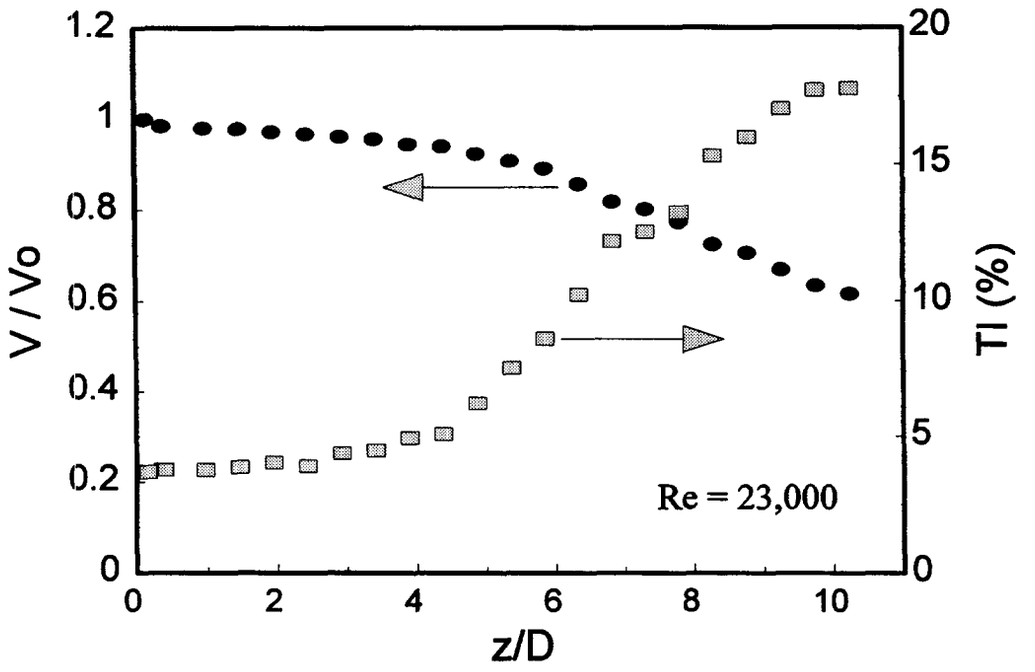

Figure 3 Hot-film measurement of the jet characteristics along the centerline

row and Lovell's suction type jet issuing out of an ASME orifice where there was no stationary ambient, and the mixing of the core of the free jet with ambient was minimum.

Radial heat transfer distributions

Effect of oblique angle. Figures 7, 8 and 9 show the detailed surface local heat transfer distributions for three different oblique angles, $\phi = 75°$, 60°, 45° for a jet-to-plate distance of seven. A better way to study these graphs is to visualize a 180° "panoramic" view of the heat transfer distribution with a standing point at the geometrical impingement point ($R = 0$) and with the viewing direction changing in 30° intervals. For the oblique angle of 75° (Figure 7), the heat transfer shows a monotonic drop from the stagnation region in a given direction ($0° \leq \theta \leq 180°$). The asymmetry of heat transfer is only apparent at a larger radial distance ($R/D > 2$) in the wall jet region. The dotted line on the plot is the result of a vertical jet ($\theta = 90°$), where heat transfer

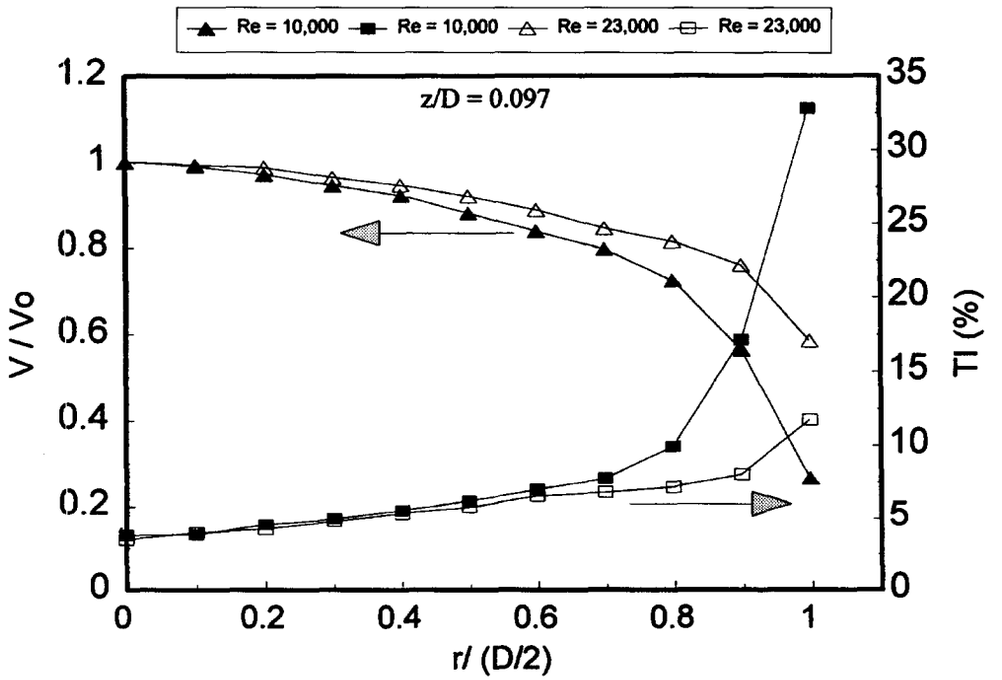

Figure 4 Profiles of velocity and turbulent intensity at the jet exit

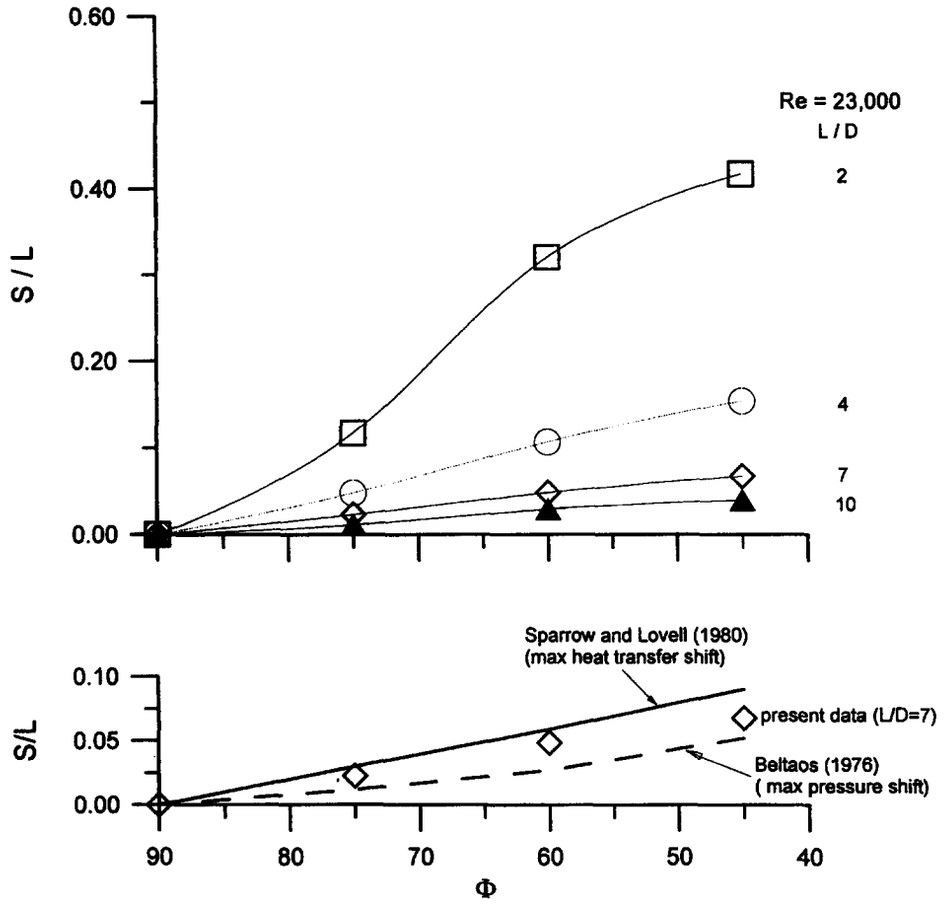

Figure 5 Scaled shift of point of maximum heat transfer

distribution is axisymmetric. The impinging jet flow suffers a change of flow direction upon impingement. The momentum loss associated with it is less on the "downhill" side, which enables flow to accelerate, and hence higher heat transfer is observed on this side.

This asymmetry of heat transfer for larger radial distances ($R/D > 2$) is more pronounced for higher inclination jets (smaller oblique angles), as shown in Figures 8 and 9, where a large scattering of heat transfer coefficients is measured. The asymmetry of heat transfer is also found in or near the stagnation region

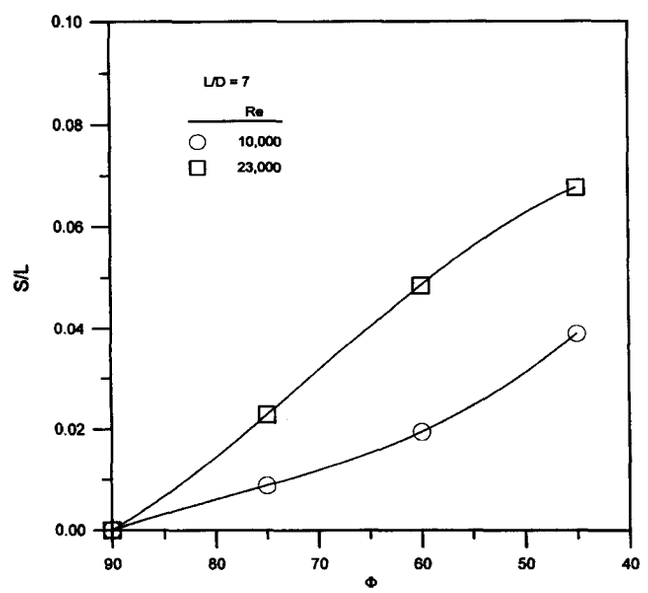

Figure 6 Reynolds number effect on the shift of maximum heat transfer

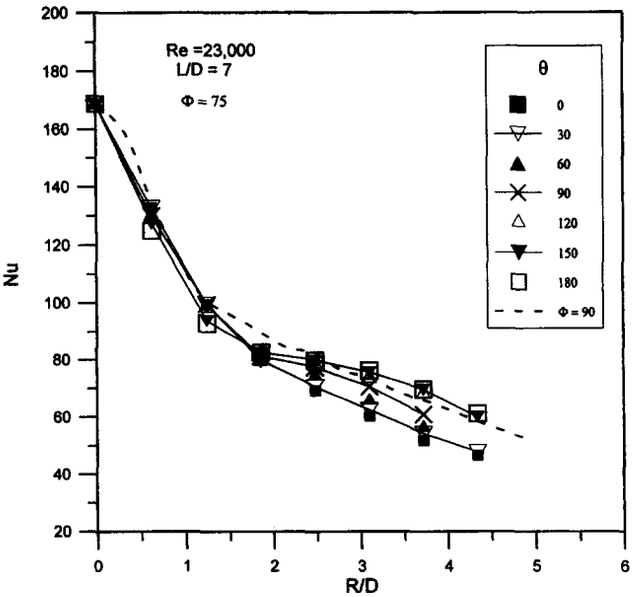

Figure 7 Radial heat transfer distributions for jet-to-plate distance $L/D=7$ and oblique angle $\phi=75°$

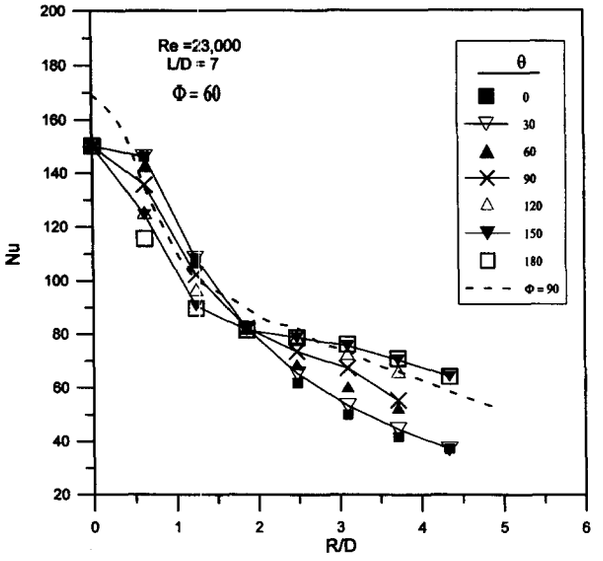

Figure 8 Radial heat transfer distributions for jet-to-plate distance $L/D=7$ and oblique angle $\phi=60°$

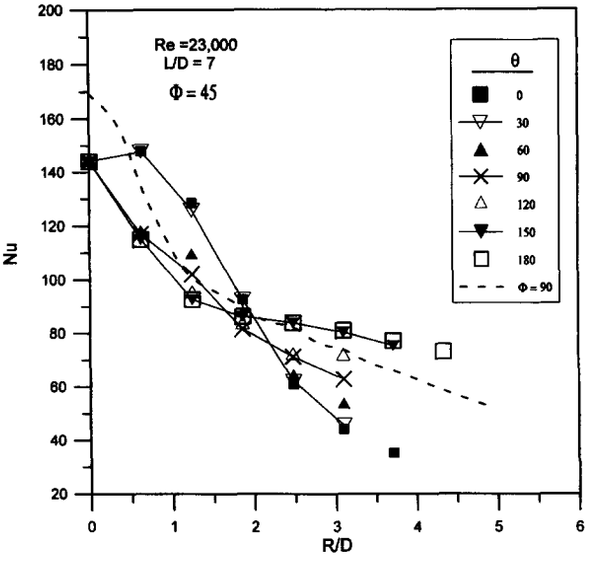

Figure 9 Radial heat transfer distributions for jet-to-plate distance $L/D=7$ and oblique angle $\phi=45°$

for $R/D < 2$. One interesting observation is that radial distance $R/D = 2$ seems to be a point of "division." In the stagnation region with $R/D < 2$, heat transfer on the "uphill" side is higher than that on the "downhill" side for the same radial distance to the geometrical impingement point. Experimental datasets flip from $R/D = 2$ on, and the opposite trend is observed when $R/D > 2$. This shows that for large L/D, where there is monotonic decrease of heat transfer in any given direction, the slope of the "surface" of heat transfer coefficients becomes less and less steep when one "travels" on the "surface" in the angular direction (θ direction). The result in this study is very similar to that of Sparrow and Lovell (1980).

One aspect of the applications of these curves is the calculation of average heat transfer over a certain surface area. The average heat transfer coefficient is proportional to the area under the distribution curves for an isothermal surface temperature. A quick qualitative assessment of the curves indicates that the deviations of average heat transfer coefficients from that of a vertical jet is small.

Effect of jet-to-plate distance. The effect of jet-to-plate distance on the local heat transfer can be seen in Figures 10–13.

Figure 10 shows the heat transfer results for Re = 23,000 at the smallest jet-to-plate distance, $L/D = 2$, and at an oblique angle of 60°. The shift of point of maximum heat transfer is clearly observed. The heat transfer distributions on the compression side showed monotonic decreasing beyond the maximum point. On the "downhill" side, however, the distributions are characteristic of that of a vertical jet for same jet-to-plate distance (Baughn and Shimizu 1988; Yan et al. 1992) with a second maximum heat transfer at the radial distance around two diameters. As a matter of fact, the distribution for $\theta = 90°$ is typical of that of a corresponding vertical jet. The second maxima of heat

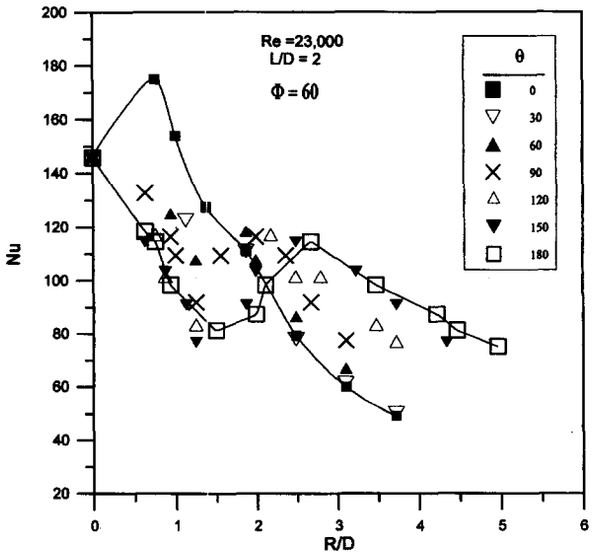

Figure 10 Radial heat transfer distributions for jet-to-plate distance $L/D=2$ and oblique angle $\phi=60°$

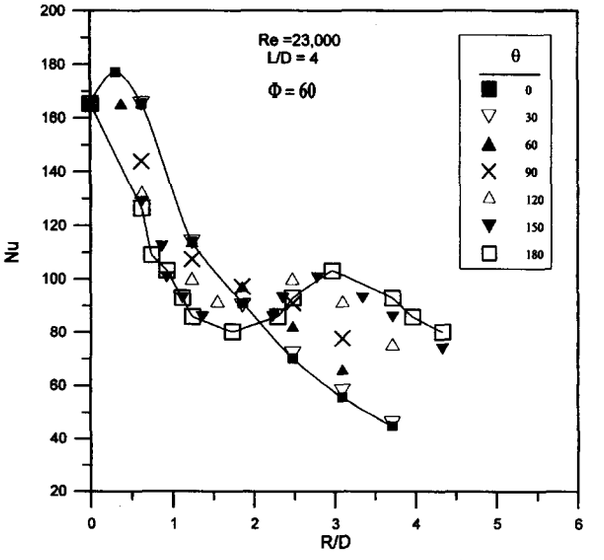

Figure 11 Radial heat transfer distributions for jet-to-plate distance $L/D=4$ and oblique angle $\phi=60°$

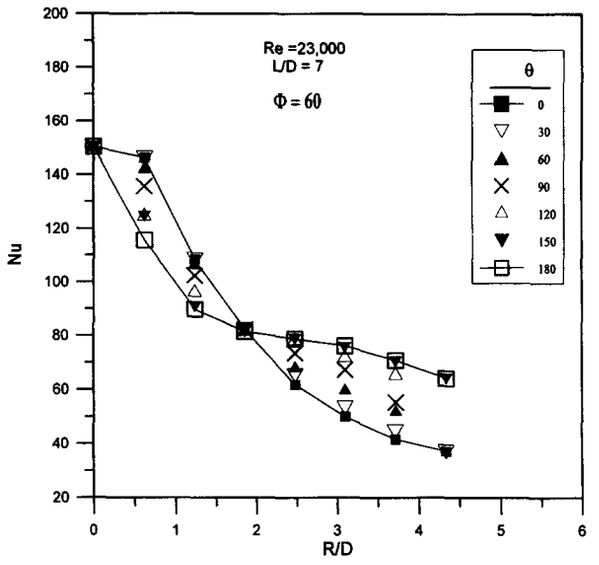

Figure 12 Radial heat transfer distributions for jet-to-plate distance $L/D=7$ and oblique angle $\phi=60°$

transfer is believed to be caused by flow transition region where the local turbulence generation is strong. Because of the strong downwash of flow from the stagnation region to the "downhill" side in which flow carries more momentum as θ angle increases, this transition is retarded to cause the delay for the point of second maximum. This strong asymmetric pattern can be easily visualized from the video tape of the experimental runs.

As the jet-to-plate distance increases (Figures 11, 12, 13), the drop of heat transfer on the compression side becomes less rapid. The figures also show that for radial distance beyond $R/D=2$, the scattering of heat transfer becomes less pronounced with the increase of jet-to-plate distance. This indicates that at the larger distances (beyond the jet potential core), the jet flow is so well mixed and spread that the heat transfer distribution on the surface is less sensitive to the jet-to-plate distance.

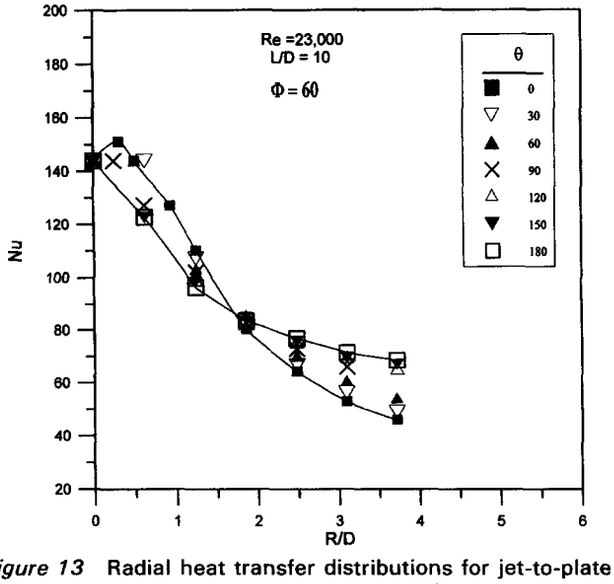

Figure 13 Radial heat transfer distributions for jet-to-plate distance $L/D=10$ and oblique angle $\phi=60°$

Conclusions

Local heat transfer distributions from an obliquely impinging circular air jet to a flat plate were obtained experimentally using the preheated wall transient liquid-crystal technique. The effects of oblique angle (ϕ) and jet-to-plate distance (L/D) on the local heat transfer were investigated for Reynolds numbers of 10,000 and 23,000. The parameter ranges are $\phi = 90°$, 75°, 60°, and 45° and $L/D = 2$, 4, 7, and 10. Conclusions are drawn as follows.

(1) Distribution of local heat transfer shows a non-axisymmetric pattern. As the jet-to-plate distance becomes smaller, the asymmetry of heat transfer distribution becomes more pronounced.

(2) In the range of parameters studied, the point of maximum heat transfer shifts from the geometrical impingement point toward the compression side of the plate. The scaled shift of maximum heat transfer increases with a decreasing oblique angle (more inclination of the jet). The shift is found to be sensitive for smaller jet-to-plate distance. This is important for design and prediction of heating or cooling of a surface with an obliquely impinging circular jet.

(3) At smallest jet-to-plate distance studied, heat transfer distribution on the compression side of the surface shows a monotonic rapid drop beyond the point of maximum, while the heat transfer distribution on the "downhill" side exhibits a same pattern as that of a vertical jet-second maxima. The location of the second maxima moves away from the center as the angular direction θ increases.

(4) It is apparent that future work of coordinate measurements of surface pressure, velocity field, and heat transfer for the same oblique impinging jet configuration is needed to resolve the issue of the relation between the point of maximum pressure, point of maximum heat transfer, and the stagnation point for an oblliquely impinging jet.

Acknowledgments

The authors would like to acknowledge the support of this study by a FUR grant from the Graduate School, Southern Illinois University at Edwardsville.

References

Baughn, J. W., Ireland, P. T., Jones, T. V. and Saniei, N. 1989. A comparison of the transient and heated-coating methods for the measurement of local heat transfer coefficients on a pin fin. *J. Heat Transfer*, **111**, 877–881

Baughn, J. W. and Shimizu, S. S. 1988. Heat transfer measurements from a surface with uniform heat flux and a fully developed impinging jet. *J. Heat Transfer*, **111**, 1096–1098

Baughn, J. W. and Yan, X. 1991. An insertion technique using the transient method with liquid crystals for heat transfer measurement in ducts. In *Fouling and Enhancement Interactions*, HTD, Vol. 164, T. J. Rabas and J. M. Chenoweth (eds.), ASME, New York, 77–83

Baughn, J. W., Yan, X. and Roby, J. L. 1994. An insertion technique using the transient method with liquid crystals for enhanced heat transfer measurements in ducts. *J. Enhanced Heat Transfer*, **1**, 179–190

Beltaos, S. 1976. Oblique impinging of circular turbulent jets. *J. Hydraulic Res.* **14**, 17–36

Camçi, C., Kim, K., Hippensteele, S. A. and Poinsatte, P. E. 1993. Evaluation of a hue capturing based transient liquid crystal method for high-resolution mapping of convective heat transfer on curved surfaces. *J. Heat Transfer*, **115**, 311–318

Carslaw, H. S. and Jaeger, J. C. 1959. *Conduction of Heat in Solids*, 2nd ed. Oxford University Press, Fair Lawn, NJ

Chuang, S. H. and Wei, C. Y. 1991. Computations for a jet impinging obliquely on a flat surface. *Int. Numer. Meth. Fluids*, **12**, 637–653

Downs, S. J. and James, E. H. 1987. Jet impingement heat transfer—A literature survey. ASME paper 87-HT-35

Gardon, R. and Akfirat, J. C. 1965. The role of turbulence in determining the heat transfer characteristics of impinging jets. *Int. J. Heat Mass Transfer*, **8**, 1261–1272

Goldstein, R. J. and Franchett, M. E. 1988. Heat transfer from a flat plate to an oblique impinging jet. *J. Heat Transfer*, **110**, 84–90

Hrycak, P. 1983. Heat transfer from round impinging jets to a flat plate. *Int. J. Heat Mass Transfer*, **26**, 1857–1865

Hwang, J. C., Tsou, F. K. and Cho, W. C. 1982. Kappa–epsilon computations of flow and heat transfer in plane oblique impinging jets. In *Comp. Method Exp. Measurements, Proc. Int. Conference*, Washington, DC, 271–282

Hwang, J. C. and Tsou, F. K. 1983. Numerical solutions for flow and heat transfer for a plane turbulent oblique impinging jet. In *Numerical Properties and Methodologies in Heat Transfer, Proceedings of the Second National Symposium*, Hemisphere, Bristol, PA, 403–417

Ichimiya, K. and Nasu, T. 1993. Heat transfer characteristics of an oblique impinging jet with confined wall. *Trans. Japan. Soc. Mech. Engineers*, Series B, **59**, 1698–1703

Ireland, P. T. and Jones, T. V. 1986. Detailed measurements of heat transfer on and around a pedestal in fully developed passage flow. *Proc. 8th Int. Heat Transfer Conference*, **3**, 975–980

Jambunathan, K., Lai, E., Moss, M. A. and Button, B. L. 1992. A review of heat transfer data for single circular jet impingement. *Int. J. Heat Fluid Flow*, **13**, 106–115

Jones, T. V. and Hippensteele, S. A. 1987. High-resolution heat-transfer-coefficient-maps applicable to compound surfaces using liquid crystals in transient wind tunnels. In *Development in Experimental Technique in Heat Transfer and Combustion*, HTD, Vol. 71, ASME, New York, 1–9

Kline, S. J. and McClintock, F. A. 1953. Describing uncertainities in single sample experiments. *Mech. Eng.* **75**, 3–8

Martin, H. 1977. Heat and mass transfer between impinging gas jet and solid surfaces. *Adv. Heat Transfer*, **13**, 1–60

Metzger, D. E., Bunker, R. S. and Bosch, G. 1991. Transient liquid crystal measurement of local heat transfer on a rotating disk with jet impingement. *J. Turbomachinery*, **113**, 52–59

Metzger, D. E. and Larson, E. E. 1986. Use of melting point surface coatings for local convective heat transfer measurements in rectangular channel flows with 90-deg. turns. *J. Heat Transfer*, **108**, 48–54

O'Brien, J. E., Simoneau, R. J., LaGraff, J. E. and Morehouse, K. A. 1986. Unsteady heat transfer and direct comparison for steady-state measurements in a rotor-wake experiment. *Proc. 8th Int. Heat Transfer Conference*, 1243–1248

Saabas, H. J., Arora, S. C. and Messeh, W. A. 1987. Application of the transient test technique to measure local heat transfer coefficients associated with augmented airfoil cooling passages. ASME paper 87-GT-212

Sparrow, E. M. and Lovell, B. J. 1980. Heat transfer characteristics of an oblique impinging circular jet. *J. Heat Transfer*, **102**, 202–209

Viskanta, R. 1993. Heat transfer to impinging isothermal gas and flame jets. *Exp. Thermal Fluid Sci.*, **6**, 111–134

Yan, X., Baughn, J. W. and Mesbah, M. 1992. The effect of Reynolds number on the heat transfer distribution from a flat plate to a turbulent impinging jet. ASME HTD, Vol. 226, 1–7

Yan, X., Baughn, J. W., Rabas, T. J. and Arman, B. 1995. A liquid-crystal transient technique for the measurements of intube local condensing heat transfer coefficients. *Exper. Heat Transfer*, **8**, 17–32

Yan, X. and Saniei, N. 1996. Measurement of local heat transfer coefficients from a flat plate to a pair of circular air impinging jets. *Exper. Heat Transfer*, **9**, 29–47